ENCIT 2018

ABCM Associação Brasileira de Engenharia e Ciências Mecânicas

17th Brazilian Congress of Thermal Sciences and Engineering
November 25th-28th, 2018, Águas de Lindóia, SP, Brazil

ENCIT-2018-0056
DESIGN OF THE GENERIC SCRAMJET COMBUSTION CHAMBER

Paulo Gilberto de Paula Toro
Ramon Carneiro
Jonatha Wallace da Silva Araújo
George Santos Marinho
Universidade Federal do Rio Grande do Norte/UFRN - Centro de Tecnologia. Av. Senador Salgado Filho, 3000 - Campus Universitário, Lagoa Nova CEP 59.078-970 – Natal/RN - Brasil
toro@ct.ufrn.br, marcossabinop@gmail.com, jonatha_wallace@hotmail.com, gmarinho@ct.ufrn.br

Gilvan Luiz Borba
Universidade Federal do Rio Grande do Norte/UFRN - Centro de Ciencias Exatas e da Terra. Av. Senador Salgado Filho, 3000 - Campus Universitário, Lagoa Nova, CEP 59.078-970 - Natal, RN - Brasil
gilvan@geofisica.ufrn.br

João Felipe de Araújo Martos
European Space Research and Technology Centre (ESTEC)-ESA, Keplerlaan 1, 2001 AZ Noordwijk, The Netherlands
Joao.Martos@esa.int

Israel da Silveira Rêgo
Instituto de Estudos Avançados/IEAv - Trevo Coronel Aviador José Alberto Albano do Amarante, nº1 Putim CEP. 12.228-001 São José dos Campos, SP - Brasil
israel.rego@ieav.ct.br

Abstract. *A generic hypersonic airbreathing propulsion based on supersonic combustion ramjet (scramjet) technology has been designed, at the Universidade Federal do Rio Grande do Norte (UFRN), using analytical theoretical analysis (engineering approach). A full-scale generic scramjet model configuration is based on the technological demonstrator scramjet 14-X S, in development at the Instituto de Estudos Avançados (IEAv). A two-dimensional hydrogen powered generic scramjet has been designed to demonstrate, in atmospheric flight, a supersonic combustion, of atmospheric air (in supersonic speed) with hydrogen, on an acceleration mission to 2050 m/s (Mach number 6.8) at 30 km geometric altitude. In this preliminary design, one-dimensional compressible flow with heat addition and one-dimensional expansion wave (Prandtl-Meyer) coupled to the area ratio theories, may describe many features of the combustor and expansion sections, respectively, of the airbreathing engine. Both theories are used to estimate the thermodynamic properties and the velocities (Mach numbers) of the supersonic atmospheric air flow. One of the most important design aspects is the temperature at the entrance of the combustion chamber because the compression must provide enough high temperature, higher than ignition temperature of the hydrogen, for supersonic combustion with the supersonic atmospheric air, at the combustion chamber. Also, the inlet air mass flow and the hydrogen mass flow rates are critical design parameters to burn, stoichiometrically, the hydrogen and the supersonic air in the combustion chamber and generating the high flow velocity at the trailing-edge of the generic scramjet to produce thrust.*

Keywords: *scramjet, supersonic combustion ramjet, hypersonic airbreathing propulsion*

1. INTRODUCTION

A 2-D full-scale generic scramjet design, to fly at approximately 2050 m/s (corresponding to Mach number 6.8) at 30 km geometric altitude (Fig. 1), is being developed at the Graduate Program in Mechanical Engineering, of Universidade Federal do Rio Grande do Norte (UFRN), in collaboration with the Instituto de Estudos Avançados (IEAv), to demonstrate in atmospheric flight the supersonic combustion, of atmospheric air (in supersonic speed) with hydrogen.

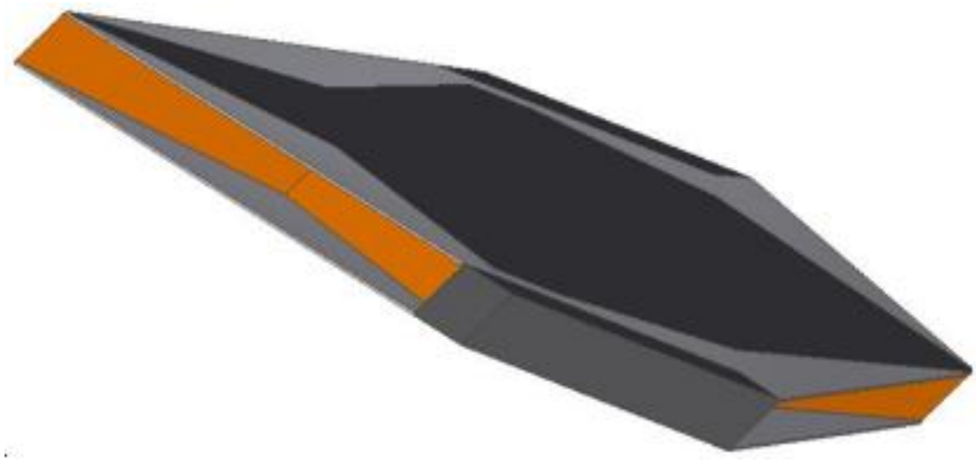

Figure 1. Schematic 2-D full-scale generic scramjet.

First, to better understand the features of the scramjet design, it is necessary to establish a nomenclature to be used. Heiser and Pratt (1994) present the terminology of the scramjet, which may be divided in three main components (Fig. 2): external and internal compression section (inlet), combustion chamber (combustor), and internal and external expansion section (outlet).

Stations 0 and 1 are the leading edges of the scramjet and of the cowl, respectively. Stations 3 and 4 are the entrance and exit of the combustion chamber. Stations 9 and 10 are the trailing edges of the cowl and the scramjet, respectively.

An important feature of the scramjet is a highly integrated system, where engine and vehicle are indistinguishable. This tight integration is caused by the fact that the front section of the vehicle contributes to the compression of atmospheric air, while the rear contributes to the generation of thrust. The net thrust produced by the scramjet is the difference between the thrust (force that propels the vehicle), generated by the expansion of exhaust gases from the rear of the engine, and the total drag (force that resists the movement of the vehicle). These forces may produce thrust to the flight of the vehicle or not depending on the balance of these forces in engine design in question.

In addition, the operation of the scramjet engine obeys the (closed) Brayton thermodynamic cycle, Heiser and Pratt (1994). The Brayton cycle points (Fig. 3) are correspondent with the reference stations of scramjet (Fig. 2). Observe that the heat addition should be evaluated as constant pressure section, because it avoids the possibility of boundary-layer separation and the necessity to design the structure to withstand the peak pressure. In order to obtain constant pressure section after fuel injection the area in this section should be divergent (Fig. 2). Also, the static pressure at the exit, station 10, of the scramjet expansion section (trailing edge) should be very close of the freestream static pressure, station 0 (Fig. 2).

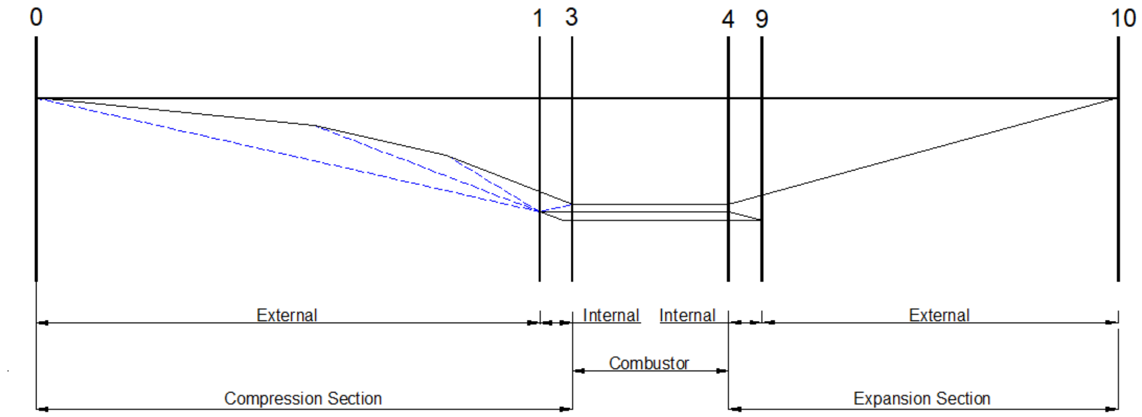

Figure 2. Airframe-integrated scramjet stations and reference terminology (adapted from Heiser and Pratt, 1994).

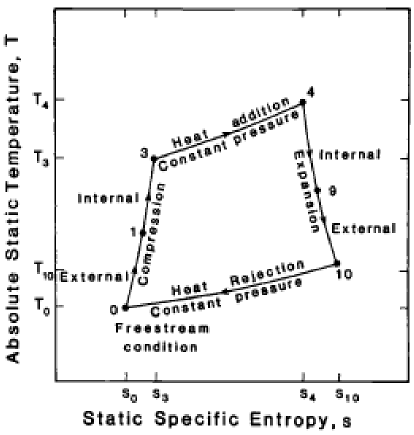

Figure 3. Brayton cycle temperature-entropy T-s diagram (Heiser and Pratt, 1994).

Finally, note that the incident shock waves (Fig. 2), from the external compression section, should incident on the leading edge of the cowl (shock on-lip) and the reflected shock wave, of the internal compression section, should incident on the entrance of the combustion chamber (shock on-corner). Therefore, the air capture area should be maximum and the length of the scramjet compression section should be minimum.

The calorically perfect gas and no effects of boundary layer assumptions are applied to this preliminary airframe-integrated generic scramjet design. Therefore, the external compression section is governed by incident shock wave, while the internal is governed by reflected shock wave. The internal and external expansion section is governed by expansion wave, Prandtl-Meyer Theory, and area ratio. The constant area section of the combustion chamber is called as isolator and is used to uniformize the flow from the compression section. Fuel is injected right after the isolator used to expand the gases from burning the fuel and the oxygen. In general, one-dimensional flow with heat addition, Rayleigh flow, is used to simulate the burning the fuel and the oxygen.

In the previous work, using analytical theoretical analysis (engineering approach), the generic scramjet air inlet design was analyzed (Toro et al., 2018), and will be integrated, in this present work, to combustion chamber and expansion section.

The generic scramjet air inlet was designed based on maximum total pressure recovery of the external compression section, to determine the deflection angles of the external compression surfaces (Toro et al. (2018). The maximum total pressure recovery, is obtained when the shock waves, established at external compression section, are of equal intensity, i.e., the Mach numbers perpendicular to the individual shock waves are equal, given, respectively, by

$$\pi = \frac{p_{te}}{p_{ti}} = \frac{p_e}{p_i}\left[\frac{\left(1+\frac{\gamma-1}{2}M_e^2\right)}{\left(1+\frac{\gamma-1}{2}M_i^2\right)}\right]^{\frac{\gamma}{\gamma-1}} \tag{1}$$

$$M_1 sen\beta_1 = M_2 sen\beta_2 = \ldots = M_{n-1} sen\beta_{n-1} \tag{2}$$

2. METHODOLOGY

In the analytical theoretical analysis, it is considering calorically perfect gas ($p = \rho RT$, $\gamma = \text{constant}$) and no boundary-layer effects (non-viscous flow). Also, the subscripts in and out are used to identify the upstream (inlet) and the downstream (outlet) conditions, respectively, of each station (Fig. 2) of the generic scramjet.

2.1 Airframe-integrated scramjet design

In consequence of the nature of the scramjet (flying at hypersonic speeds), they are unable to produce thrust while stationary. Solid-rocket engines may be used to accelerate the scramjet to a speed such that the shock waves produced by the air intake are able to compress the atmospheric air achieving the operational conditions (Hass et al., 2005). Such approach may provide an affordable path for maturing Brazilian hypersonic airbreathing components and subsystems in flight. The Brazilian hypersonic accelerator vehicle which is composed by two-stage (S31 and S30) solid rocket engines, unguided, rail launched, is able to accelerate the generic scramjet to the predetermined flight test conditions of the scramjet operation (30 km altitude at Mach number 6.8) from one of the Brazilian Launch Centers (Centro de Lançamento de Alcântara, CLA, or Centro de Lançamento da Barreira do Inferno, CLBI).

So, the first step is to determine the dimensions of the generic scramjet (Fig. 4), which will be coupled at the diameter of the rocket engine (Fig. 5).

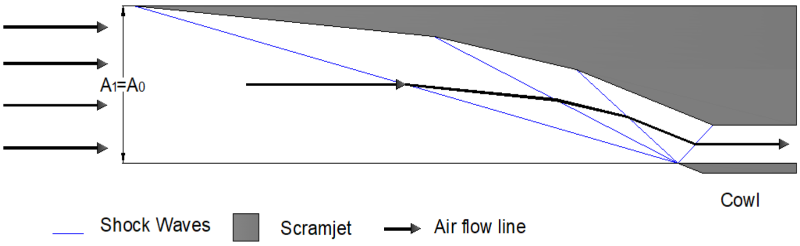

Figure 4. Captured area of the scramjet air inlet considering shock on-lip e shock on-corner.

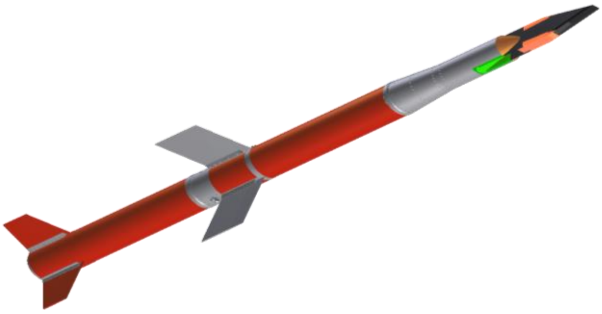

Figure 5. Generic scramjet coupled to the hypersonic accelerator vehicle.

Respecting shock on-lip and shock on-corner design conditions, the mass conservation law for the (external and internal compression section) control volume may be used to obtain the height of the combustion chamber and the location of the leading edge of the cowl:

$$\dot{m} = \rho_0 u_0 A_0 = \rho_3 u_3 A_3 \tag{3}$$

2.2 Combustor section (one-dimensional flow with heat addition)

One-dimensional flow with heat addition, Rayleigh Flow, (Fig. 6) may be applied to combustion process which occurs between the entrance (inlet) and the exit (outlet) of the scramjet combustor (Fig. 2). The governing equations are given by (Anderson, 2003)

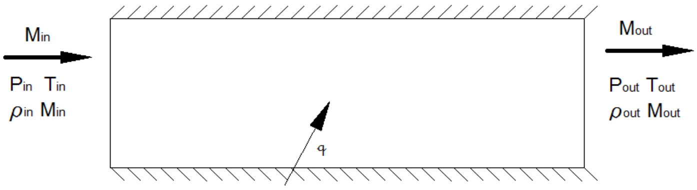

Figure 6: Rayleigh Flow, one-dimensional with constant-area heat addition.

$$\rho_{in}\ u_{in} = \rho_{out}\ u_{out} \tag{4}$$

$$p_{in} + \rho_{in} u_{in}^2 = p_{out} + \rho_{out}\ u_{out}^2 \tag{5}$$

$$h_{in} + \frac{u_{in}^2}{2} + q = h_{out} + \frac{u_{out}^2}{2} \tag{6}$$

The conditions at the entrance of the combustion chamber (subscripts in) are known, given by the thermodynamic properties and speed (Mach number) estimated just right after the reflected shock wave at the internal compression section (Fig. 2). For the calorically perfect gas and no boundary-layer effects analytical relationships for one-dimensional flow with heat addition may be found.

The energy equation (Eq. 6) indicates the heat addition change the total energy (temperature), obtained by

$$q = c_p \left(T_{o,\,out} - T_{o,\,in} \right) \tag{7}$$

where: the total temperature is given by:

$$\frac{T_o}{T} = 1 + \frac{\gamma - 1}{2} M^2 \tag{8}$$

Closed-form of the thermodynamic property (static pressure, static density and static temperature, total temperature) ratios across constant-area heat addition may be obtained by manipulating the momentum equation, and they are given by:

$$\frac{p_{out}}{p_{in}} = \left(\frac{1 + \gamma\, M_{in}^2}{1 + \gamma\, M_{out}^2} \right) \tag{9}$$

$$\frac{\rho_{out}}{\rho_{in}} = \left(\frac{1 + \gamma\, M_{out}^2}{1 + \gamma\, M_{in}^2} \right) \left(\frac{M_{in}}{M_{out}} \right)^2 \tag{10}$$

$$\frac{T_{out}}{T_{in}} = \left(\frac{1 + \gamma\, M_{in}^2}{1 + \gamma\, M_{out}^2} \right)^2 \left(\frac{M_{out}}{M_{in}} \right)^2 \tag{11}$$

$$\frac{T_{o,out}}{T_{o,in}} = \left(\frac{1 + \gamma\, M_{in}^2}{1 + \gamma\, M_{out}^2} \right)^2 \left(\frac{M_{out}}{M_{in}} \right)^2 \left(\frac{1 + \frac{\gamma - 1}{2} M_{out}^2}{1 + \frac{\gamma - 1}{2} M_{in}^2} \right) \tag{12}$$

Note the flow from the external and internal compression section are deflected to the combustor entrance (Fig. 2) at supersonic speed (at constant pressure, constant density, constant temperature and constant Mach number). Fuel (H_2) will be injected right after the entrance station (Fig. 2) in (minimal) sonic speed. Rayleigh flow (one-dimensional flow with heat addition) may be applied to the combustion process to burn H_2 and O_2 in supersonic speed, resulting at the exit of the combustor chamber (outlet) an increase in static pressure, static density, static temperature and a decrease the Mach number (speed) of the combustion product flow.

The conditions at the entrance of the combustion chamber are known, given by the thermodynamic properties and speed (and corresponding Mach number) estimated by Toro et al. (2018) just right after the reflected shock wave (Mach number 2.55 and temperature of 1008 K) at the internal compression section (Fig. 2).

2.3 Combustor section (burn hydrogen with supersonic airflow)

The stoichiometric fuel/air ratio may be evaluated from the basic principles of chemical reactions, where the general chemical expression for the complete combustion, is given by

$$f_{st} = \frac{36x + 3y}{103(4x + y)} \tag{13}$$

where: for hydrogen (H_2) $x = 0 \; and \; y = 2$ (Heiser e Pratt, 1994). Therefore, the stoichiometric combustion of hydrogen H_2 and the atmospheric air (O_2 oxygen) $f_{st} = 0.0291$.

Also, the ratio of fuel mass flow rate to air mass flow rate, fuel/air ratio *f*, is an indicator of the combustion conditions in the burner (Heiser e Pratt, 1994), which may be defined as

$$f = \frac{\dot{m}_{\mathrm{fuel}}}{\dot{m}_{\mathrm{air}}} \tag{14}$$

where: $\dot{m}_{\text{air}}$ and $\dot{m}_{\text{fuel}}$ are the inlet air mass flow rate, $\dot{m}_{air}^{inlet} = \rho_0 \; u_0 \; A_0$, and the fuel mass flow rate, respectively.

Combining Eq. 12 and Eq. 13, the fuel mass flow rate $\dot{m}_{fuel}$ may be evaluated by

$$\dot{m}_{fuel} = f_{st} \;\; \dot{m}_{air} \tag{15}$$

The chemical energy rate available to the scramjet engine is given by (Heiser e Pratt, 1994)

$$\text{chemical energy rate} = \dot{m}_{\text{fuel}} \;\; h_{pr} \tag{16}$$

where: h_{pr} is the heats of reaction, and for hydrogen is $119{,}954{,}000 \; [\text{J/kg fuel}]$ (Heiser and Pratt, 1994).

2.4 Internal and external expansion section (expansion wave)

The expansion wave (Prandtl-Meyer) theory may be applied to the internal and external expansion section (Fig. 2). When the supersonic flow is turned into itself (Fig. 7) an isentropic expansion wave is established at the deflection angle, and the expansion wave is limited by the head and tail of the expansion wave defined by the Mach angle μ_{head}, μ_{tail}, respectively, which are given by (Anderson, 2003).

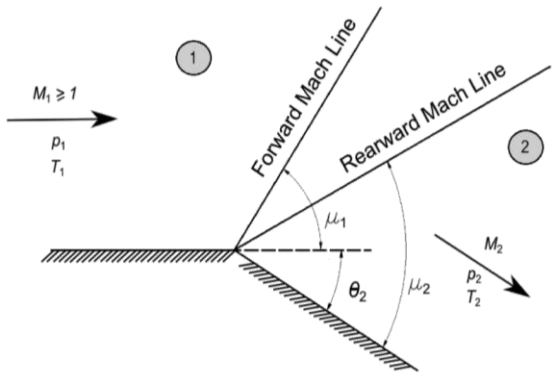

Figure 7: Expansion wave geometry.

$$\mu_{head} = \text{arcsen}\left(\frac{1}{M_{in}}\right) \tag{17}$$

$$\mu_{tail} = \text{arcsen}\left(\frac{1}{M_{out}}\right) \tag{18}$$

The expansion deflection angle θ_{e} is given by the Prandtl-Meyer function $\upsilon(\text{M})$:

$$\theta_e = \upsilon(M_{out}) - \upsilon(M_{in}) \tag{19}$$

where the Prandtl-Meyer function $\upsilon(\text{M})$, which is function of the Mach number, is given by:

$$\upsilon(M) = \sqrt{\frac{\gamma+1}{\gamma - 1}} \;\; tg^{-1} \sqrt{\frac{\gamma-1}{\gamma+1}\left[M^2 - 1\right]} - tg^{-1}\sqrt{M^2 - 1} \tag{20}$$

Once Mach number after expansion wave M_{out} is determined the closed form of the thermodynamic property (static pressure, static density and static temperature) ration across the expansion wave may be obtained by the isentropic relationships given by (Anderson, 2003)

$$\frac{T_{out}}{T_{in}} = \left(\frac{1 + \frac{\gamma - 1}{2} M_{in}^2}{1 + \frac{\gamma - 1}{2} M_{out}^2} \right) \tag{21}$$

$$\frac{p_{out}}{p_{in}} = \left(\frac{T_{out}}{T_{in}} \right)^{\frac{\gamma}{\gamma - 1}} \tag{22}$$

$$\frac{\rho_{out}}{\rho_{in}} = \frac{p_{out}}{p_{in}} \frac{T_{in}}{T_{out}} \tag{23}$$

Note the flow across the expansion wave promote a decrease of static pressure, static density, static temperature, and an increase of Mach number. The flow remains supersonic and parallel to the flat surface of the internal and external expansion section (Fig. 2) of the hypersonic vehicle with airframe-integrated scramjet engine lower surface.

2.5 Area ratio (expansion wave)

If the supersonic flow, which establishes the expansion wave, is confined (Fig. 8), the head Mach wave strikes the lower surface of this confined environment and is reflected toward the upper surface. In this case the Prandtl-Meyer theory is not valid any more, and the area ratio should be applied (Heiser and Pratt, 1994). The reflected head Mach wave is assumed to be the same as the incident head Mach wave, which is given by

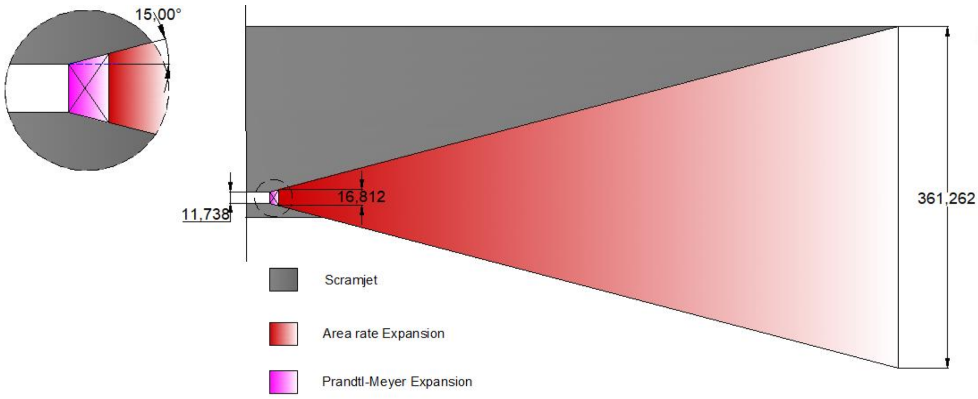

Figure 8: Confined expansion wave geometry.

$$\frac{A_{out}}{A_{in}} = \frac{M_{in}}{M_{out}} \left(\frac{1 + \frac{\gamma - 1}{2} M_{out}^2}{1 + \frac{\gamma - 1}{2} M_{in}^2} \right)^{\frac{\gamma + 1}{2(\gamma - 1)}} \tag{24}$$

3. RESULTS AND COMMENTARIES

The thermodynamic properties of the air at 30 km geometric altitude (Tab. 1), where the scramjet vehicle (Fig. 1) is flying in hypersonic velocity of approximately 2050 m/s (corresponding to Mach number 6.8), are obtained from The U.S. Standard Atmosphere (1976).

Table 1. Earth's atmospheric thermodynamic properties at 30 km altitude (U.S. Standard Atmosphere, 1976).

Altitude	Temperature	Pressure	Density	Sound speed
km	K	Pa	kg/m^3	m/s
30	226.5	1197	0.01841	301.7

First, the deflection angles of the external compression surfaces (Fig. 9) were found using the optimization criteria of maximum total pressure recovery π (Eq. 1) which satisfy $M \; sen\beta$ across each incident shock wave (Eq. 2). Right after, the thermodynamic properties and the velocities (Mach numbers) of the airflow, at the generic scramjet inlet, were evaluated by applying the one-dimensional compressible flow (shock wave) theory, considering calorically perfect gas and no boundary layer effects (Toro et al., 2018). Mach number 2.55 (corresponding to speed of 1624 [m/s]) and the static temperature of 1008 [K] of supersonic airflow at the entrance of the combustion chamber were found.

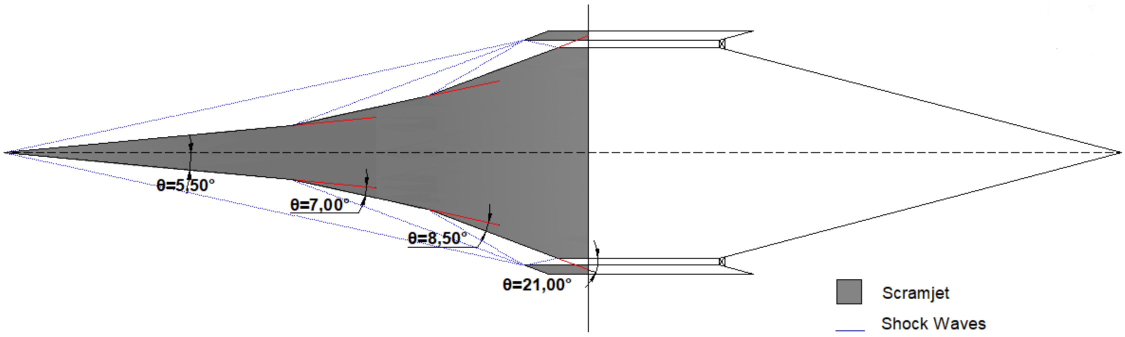

Figure 9. Generic scramjet flying at Mach number 6.8, to demonstrate supersonic combustion at 30 km altitude.

First, the heat addition, at the combustor section due to burning the hydrogen and atmospheric air in supersonic speed, and fuel mass flow rate were evaluated. The (captured area of the scramjet) air inlet height was defined to be 0.373 [m], therefore, for constant width, the combustor height evaluated by Eq. 3 is 0.0235 [m]. The inlet and the combustor air mass flow rates are equal to 1.6906 [kg/s]. To avoid the chocked flow after combustion, it is assumed the combustion products is supersonic as Mach number 1.2. For this case, the heat addition (Eq. 7) necessary to stoichiometrically burn the hydrogen is 1,543,945 [J/kg air]. The fuel mass flow rate is 0,01287 [kg/s] evaluated by Eq. 16, where the chemical energy rate is assumed as the heat addition by the supersonic airflow at the entrance of the combustor.

After, it was applied the Prandtl-Meyer theory and was determined the length of this theory is valid, considering the expansion wave that occurs at the expansion section of the scramjet and of the cowl (Fig. 8). The reflected expansion wave related to head of the expansion Mach angle is the same as the incident head of the expansion Mach angle, given by Eq. 17.

For the length from the head of the incident to reflected Mach angle was applied the Prandtl-Meyer theory (Eqs. 19-20), after the area ratio was applied (Eq. 24) and the conditions at the trailing-edge of the scramjet (point 10, Fig. 2) were determined (Tab. 2), for two cases: expansion deflection angles of 10º and 15º. For both cases the isentropic relationships were applied to determine the thermodynamic properties.

Table 2. Thermodynamic properties at the generic scramjet engine inlet, non-viscous flow, calorically perfect gas ($p = \rho RT$, $\gamma = 1.4$).

					$\theta_{Expansion} = 10^o$		$\theta_{Expansion} = 15^o$	
		Freestream	Combustor entrance (Toro et al. 2018)	Combustor exit	Expansion section (Prandtl-Meyer)	Expansion section (area ratio)	Expansion section (Prandtl-Meyer)	Expansion section (area ratio)
M		6.8	2.55	1.20	1.556	5.36	1.73	5.2
$\frac{p_{out}}{p_{in}}$				3.3518	0.6088	0,0050	0.4727	0,0077
$\frac{T_{out}}{T_{in}}$				2.4864	0.8668	0,2200	0.8070	0,2490
$\frac{\rho_{out}}{\rho_{in}}$				1.3481	0.7015	0.0227	0.5855	0.0309
p	Pa	1197	106,991.30	358,612	218,313	1,090	169,520	1,305
T	K	226.5	1008.64	2507	2176	478.84	2024	504.09
ρ	kg/m^3	0.01841	0.36952	0.49813	0.34945	0.00793	0.2917	0.0090

a	m/s	301.7	636.67	1003	935	438.67	902	450.09
u	m/s	2051.6	1624.01	1204	1455	2351.29	1556	2340.47
T_{total}	K		2321.14	3230	3230	3230	3230	3230

It is important to point out, the generic scramjet, with three ramps at the compression section (Fig. 9), with leading-edge angle of 5.5º, followed by two deflection angles of 7º and 8.5º, flying at 30 km of geometric altitude with speed corresponding at Mach number 6.8 is capable to generate a supersonic velocity corresponding to Mach number of 2.55 and a static temperature (Toro et al., 2018) higher than 845.15 K, ignition temperature of hydrogen, at the entrance of combustion chamber (Tab. 2). Also, in order to avoid the chocked flow after combustion, it is assumed the Mach number 1.2 at the combustion chamber exit.

One may realize the flow across the expansion wave promote a decrease of static pressure, static density, static temperature, and an increase of Mach number (and the correspondent flow velocity).

Besides the Mach number at the scramjet trailing-edge is lower than the Mach number at the scramjet leading-edge, for both cases, expansion deflection angles of 10º and 15º, the flow velocity at the scramjet trailing-edge is higher than the Mach number at the scramjet leading-edge. Therefore, able to produce thrust.

The thermodynamic properties and airflow Mach number from tip-to-tail, of the generic scramjet flying at 30 km altitude with Mach number 6.8 (2050 m/s), are estimated applying the one-dimensional compressible flow (shock wave) theory, one-dimensional flow with heat addition and the one-dimensional compressible flow (expansion wave) theory coupled to the area ratio to the compression, combustor and expansion sections, respectively (Figs. 10 and 11), considering no effects of boundary layer and the airflow behaves as calorically perfect gas.

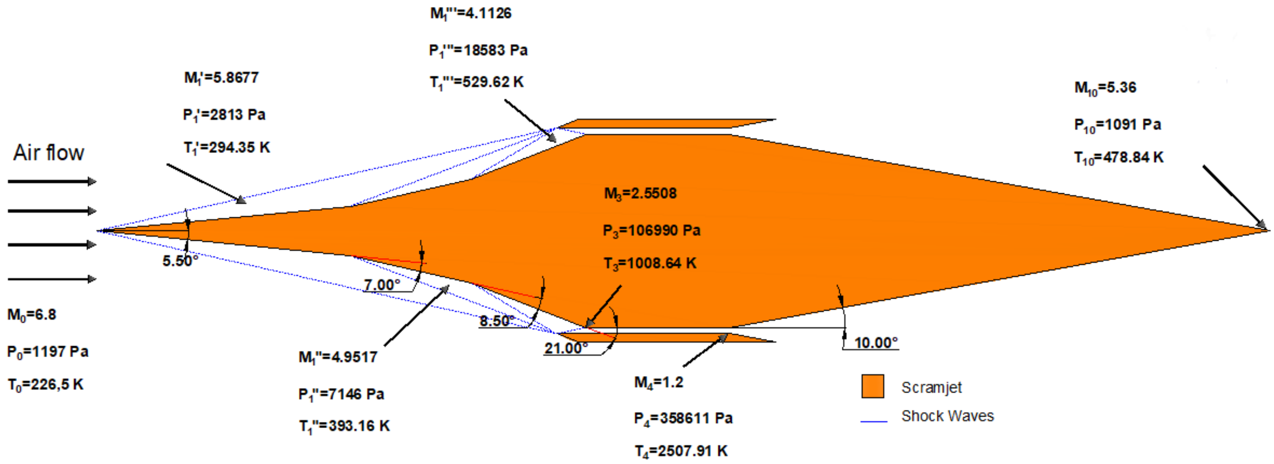

Figure 10. Thermodynamic properties from tip-to-tail of the generic scramjet inlet, for expansion deflection angle 10º.

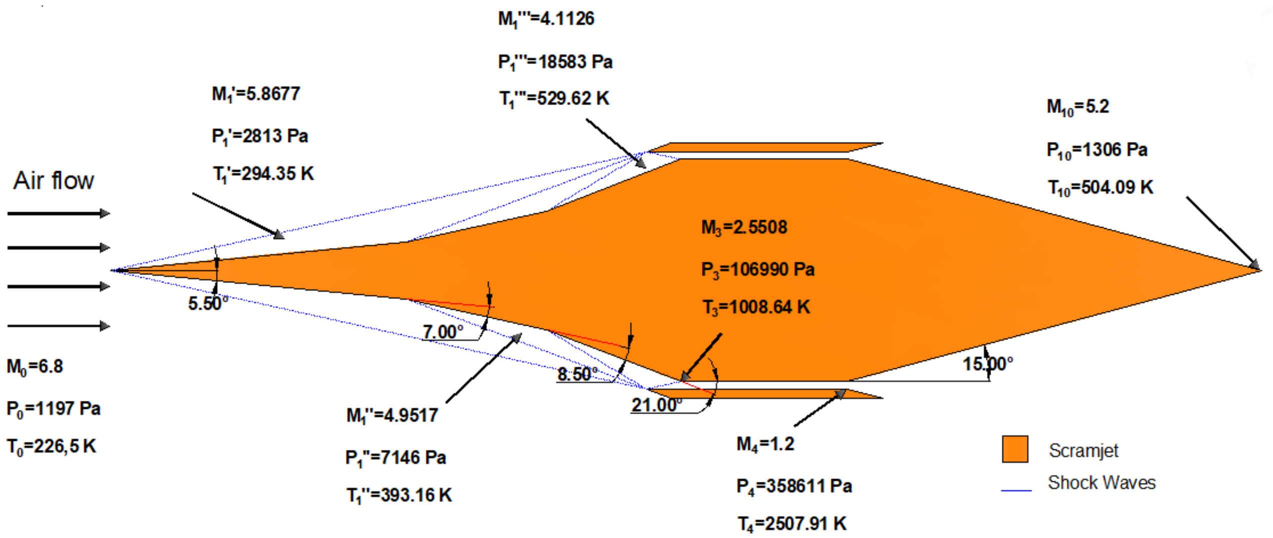

Figure 11. Thermodynamic properties from tip-to-tail of the generic scramjet inlet, for expansion deflection angle 15º.

4. CONCLUSION AND OUTLOOK FOR FUTURE PROJECTS

A 2-D full-scale generic scramjet design, to fly at approximately 2050 m/s (corresponding to Mach number 6.8) at 30 km geometric altitude (Fig. 1), is being developed at the Graduate Program in Mechanical Engineering, of Universidade Federal do Rio Grande do Norte (UFRN), in collaboration with the Instituto de Estudos Avançados (IEAv), to demonstrate in atmospheric flight the supersonic combustion, of atmospheric air (in supersonic speed) with hydrogen.

The theoretical analytical methodology using one-dimensional compressible flow (shock wave) theory, one-dimensional flow with heat addition and the one-dimensional compressible flow (expansion wave) theory coupled to the area ratio were applied to design the compression, combustor and expansion sections of the generic scramjet, respectively, considering no effects of boundary layer and calorically perfect gas airflow.

For a given scramjet air inlet configuration the methodology present in this work is capable of evaluating the thermodynamic properties and Mach numbers (corresponding to flow velocities) of the leading-edge to trailing-edge of the generic scramjet.

The compression section compound by three ramps with turning angle of 5.92º, 6.98º and 8.22º, optimized by the total pressure recovery and the strength of shockwave criteria, deliver 1.6906 kg/s of air and 1,543,945 J/kg to burn 0,01287 kg/s of hydrogen at the combustor section. The combustion products are expanding, through the expansion deflection angle of 10º, to 2351.29 m/s higher than the generic scramjet velocity of 2050 m/s, generating, probably, thrust.

In the future work, not only the high temperature effects but also the viscous effects will be considering in the design of this generic scramjet configuration.

5. ACKNOWLEDGEMENTS

The first five authors would like to thanks to Universidade Federal do Rio Grande do Norte (UFRN) the support given to complete this scientific work. The first author (as Visiting Professor) would like to express appreciation to UFRN the possibility to apply the knowledge in aerothermodynamics and hypersonics in the research area in hypersonic airbreathing propulsion based on supersonic combustion ramjet (scramjet) technology. This work has been partially sponsored by European Space Research and Technology Centre (ESTEC) and the sixth author would like to extend his appreciation to support this project. Finally, a portion of this effort was supported by Instituto de Estudos Avançados (IEAv) and by the Propulsão Hipersônica 14-X (PropHiper) Project and the last author would like express his appreciation.

6. REFERENCES

Anderson, J. D., Modern Compressible Flow, The Historical Perspective. McGraw-Hill, Inc., ed. 2nd, 2003.

Heiser, W. H.; Pratt, D. T. Hypersonic Airbreathing Propulsion. Washington, D.C, American Institute of Aeronautics and Astronautics, 1994.

Toro, P. G. P.; Carneiro, R.; Araújo, J. W. S.; Marinho, G. S.; Borba, G. L.; Rego, I. S.; Martos, J. F. A., "Design and Analysis of a generic scramjet air inlet". 17th Brazilian Congress of Thermal Sciences and Engineering (ENCIT 2018-0751). November 25th-28th, 2018, Águas de Lindóia, SP, Brazil.

U.S. Standard Atmosphere. NASA TM-X 74335. National Oceanic and Atmospheric Administration, National Aeronautics and Space Administration and United States Air Force. 1976.

7. RESPONSIBILITY NOTICE

The authors are the only responsible for the printed material included in this scientific article.

The authors declare that there is no conflict of interest regarding the publication of this scientific article.